Tracking Local Conformational Changes of Ribonuclease A Using Picosecond Time-Resolved Fluorescence of the Six Tyrosine Residues

Melinda Noronha,*† João C. Lima,‡ Emanuele Paci,§ Helena Santos,† and António L. Maçanita*
*Centro de Química Estrutural, Instituto Superior Técnico, Universidade Técnica de Lisboa, Lisbon, Portugal; †Instituto de Tecnologia Química e Biológica, Universidade Nova de Lisboa, Oeiras, Portugal; ‡REQUIMTE/CQFB, Faculdade de Ciências e Tecnologia, Universidade Nova de Lisboa, Caparica, Portugal; §Department of Physics and Astronomy, University of Leeds, Leeds, United Kingdom

ABSTRACT The six tyrosine residues of ribonuclease A (RNase A) are used as individual intrinsic probes for tracking local conformational changes during unfolding. The fluorescence decays of RNase A are well described by sums of three exponentials with decay times ($\tau_1 = 1.7$ ns, $\tau_2 = 180$ ps, and $\tau_3 = 30$ ps) and preexponential coefficients ($A_1 = 1$, $A_2 = 1$, and $A_3 = 4$) at pH 7, 25°C. The decay times are controlled by photo-induced electron transfer from individual tyrosine residues to the nearest disulphide (–SS–), bridge, which is distance (R) dependent. We assign τ_1 to Tyr-76 ($R = 12.8$ Å), τ_2 to Tyr-115 ($R = 6.9$ Å), and τ_3 to Tyr-25, Tyr-73, Tyr-92, and Tyr-97 (all four at $R = 5.5 \pm 0.3$ Å) at 23°C. On the basis of this assignment, the results show that, upon thermal or chemical unfolding only Tyr-25, Tyr-92, and Tyr-76 undergo significant displacement from their nearest –SS– bridge. Despite reporting on different regions of the protein, the concordance between the transition temperatures, T_m, obtained from Tyr-76 ($T_m = 59.2$°C) and Tyr-25 and Tyr-92 ($T_m = 58.2$°C) suggests a single unfolding event in this temperature range that affects all these regions similarly.

INTRODUCTION

Fluorescence spectroscopy is widely used as a tool for protein folding studies (1). When multiple tryptophan (Trp) or tyrosine (Tyr) residues are present, the steady-state fluorescence is the sum of the signals from all the fluorescent residues, located in different parts of the protein. Time-resolved fluorescence spectroscopy (TRFS) has the potential to track several Trp/Tyr residues given that the decay times can be attributed to individual residues.

The use of TRFS has been hindered, in part, because several studies have shown the appearance of more than one decay time for proteins with a single Trp (2) or Tyr (3) residue. However, we have recently shown that the fluorescence of *Staphylococcus aureus* nuclease A (SNase), with a single Trp (4), and that of bovine ubiquitin (UBQ), with a single tyrosine (Tyr) residue (5), decay as a single exponential below the unfolding temperature region. Above this temperature region, the decays become multiexponential due to the fluorescence contribution of the unfolded protein, and from the preexponential coefficients of these decays, the mol fractions of the folded and unfolded proteins could be accurately evaluated and used to calculate equilibrium constants, enthalpies, entropies, and specific heats of unfolding.

In this work, we explored the application of TRFS to discriminate the fluorescence signal of the multichromophoric protein, ribonuclease A (RNase A), and to track local conformational changes resulting from thermal and chemical unfolding. RNase A was selected because it is a benchmark protein for biophysical studies, being one of the most well-characterized proteins (6,7). Furthermore, some studies have employed site-directed mutagenesis to introduce Trp residues in different parts of the protein (8), thus providing information in the site-specific region around the Trp residue in the mutant. However, these substitutions can result in structural changes with respect to the wild-type protein, as indirectly observed on comparison of changes in the thermodynamic properties associated with the unfolding process such as the transition temperature (T_m), enthalpy (ΔH), and entropy (ΔS) (8). Consequently, the possibility of obtaining information on the sites around the six Tyr residues in the unaltered protein would be beneficial.

The results of this work allowed us to assign the fluorescence decay times of the multiexponential decays of RNase A to its different Tyr residues. We also concluded that electron transfer is the mechanism responsible for the observed short decay times. Finally, on the basis of the assignment, we were able to use TRFS to probe the conformational changes, resulting from thermal and chemical unfolding that occur in the different regions where the Tyr residues are located and couple the experimental data to molecular dynamic (MD) simulations.

EXPERIMENTAL

Sample preparation

Bovine pancreatic ribonuclease A (M_w = 13,700 Da) was purchased from Boehringer Mannheim (Basel, Switzerland) and from Sigma (ribonuclease A type XII-A; St. Louis, MO) and dialyzed against 10 mM sodium phosphate, pH 7.3. Protein concentration was determined by optical spectroscopy, with an extinction coefficient of 9800 $Lmol^{-1}cm^{-1}$ at 278 nm. Guanidine hydrochloride (99% pure) was purchased

Submitted July 19, 2006, and accepted for publication February 1, 2007.

Address reprint requests to António L. Maçanita, Instituto Superior Técnico, Av. Rovisco Pais, 1049-001 Lisboa, Portugal. Tel.: 351-21-8419606; E-mail: macanita@ist.utl.pt.

0006-3495/07/06/4401/14 $2.00

doi: 10.1529/biophysj.106.093625

from Fluka (Milwaukee, WI). Sodium dihydrogen phosphate and disodium hydrogen phosphate were of analytical grade and were purchased from Merck (Rahway, NJ). *N*-acetyl-tyrosinamide (NAYA) was purchased from Sigma.

Absorption and fluorescence spectroscopy

Ultraviolet (UV)-absorption spectra were measured on an Olis (Bogart, GA) UV-Vis DW2 double-beam spectrophotometer with 1.0 nm resolution equipped with a circulating water bath and a thermocouple placed inside the cell for temperature control. Steady-state fluorescence excitation and emission spectra were measured using a SPEX (Edison, NJ) Fluorog 212I spectrofluorimeter. All spectra were collected in the sample-to-reference (S/R) mode and corrected for optics, detector wavelength dependence (emission spectra), and lamp intensity wavelength dependence (excitation spectra). Fluorescence was collected in right angle geometry.

Fluorescence quantum yield of RNase A, at pH 7 and at 25°C, was determined by comparison to parent compound *N*-acetyl-tyrosinamide (NAYA), whose quantum yield was in turn determined using a standard solution of *p*-terphenyl in cyclohexane (0.77) (9).

Time-resolved fluorescence measurements were carried out using the single-photon counting technique as previously described (10). Excitation of samples was carried out with the frequency-tripled output of an actively mode-locked picosecond Ti-Sapphire laser (Spectra Physics Tsunami; Mountain View, CA), pumped by a solid-state laser (Spectra Physics Millennia Xs). The repetition rate was set to 4 MHz by passage through an optical-acoustic modulator (Pulse Selector 3980, Spectra Physics). Light pulses were monitored with a fast photodiode, filtered with a constant fraction discriminator (Canberra 2126), and used as stop signals in a time-to-amplitude converter (Canberra 2145 TAC). Excitation was vertically polarized and emission was collected at 90° geometry, passed through a polarizer at ~54.7° (Spindler & Hoyer (Göttingen, Germany) Glan-Thompson laser prism polarizer, Franklin, MA) and a monochromator (Jobin-Yvon (Longjumeau, France) H20 Vis;), and detected with a microchannel plate photomultiplier (MCP-PT Hamamatsu R3809u-50; Hamamatsu, Japan). Inverted START-STOP configuration was used in the acquisition. The experimental instrumental response function for all excitation wavelengths was in the 38–42-ps range. Alternate collection of pulse profile and sample decays was performed (10^3 counts at the maximum per cycle) until $\sim 5 \times 10^3$ (typical) to 3×10^4 total detected counts had been accumulated at the maximum of the fluorescence signal. The fluorescence decays were deconvoluted on a PC, using Striker's SAND program (11) (LINUX version), which allows individual and global analysis of the decays with individual shift optimizations.

Molecular orbital calculations

Gas phase ionization potentials (*IP*) and electron affinities (*EA*) were calculated from the formation enthalpies of the molecule and of its oxidized and reduced forms, respectively (12). Molecular geometries were first calculated using the MM^+ molecular mechanics method and then optimized with the semiempirical AM1 method at the UHF level, using HyperChem version 5.0 software by Hypercube (Gainesville, FL) (13). Enthalpies of formation were obtained by AM1 from single point calculations on the optimized geometries.

Molecular dynamics

Simulations were performed with the program CHARMM (14) using the all-atom force-field CHARMM22 (15) and a generalized Born continuum model to include the effects of the solvent (16). Starting from the x-ray crystal structure, 1FS3 (17), we first performed a short steepest descent minimization to remove possible steric clashes, followed by a slow heating to the desired temperatures, and then performed canonical simulations lasting between 2 and 10 ns. The temperatures chosen were 23, 87, and 177°C. At 23°C, the protein remains stable and the root mean-square deviation (RMSD) reaches a plateau at ~2.5 Å after 0.5 ns and never exceeds 3 Å during the whole duration of the simulation (4 ns). At the higher temperatures, the RMSD increases, but the protein never completely unfolds due to the presence of the four disulphide bonds. At 177°C, the RMSD from the native structure is, on average, 5.5 Å and never exceeds 7 Å. Langevin dynamics were used with a low friction coefficient to accelerate the sampling relative to a water-like friction. The integration step was 2 fs for all of the simulations performed.

RESULTS

Absorption and steady-state fluorescence of RNase A

The absorption and emission spectra of RNase A at pH 7.2 and 23°C (Fig. 1 *a*) show maximum absorption at $\lambda_{max} = 278$ nm and maximum emission at $\lambda_{em} = 306$ nm. The absorption spectrum is 1 nm blue-shifted with respect to NAYA in the nonpolar solvent dioxane ($\lambda_{max} = 279$ nm) and 3 nm red-shifted with respect to NAYA in water ($\lambda_{max} = 275$ nm) (9).

The maximum fluorescence emission of NAYA varies between $\lambda_{max} = 303$ nm in dioxane and $\lambda_{em} = 305$ nm in water; hence, RNase A shows a slight red shift in comparison to NAYA in water. The fluorescence quantum yield of RNase A at 23°C ($\phi_F = 0.013 \pm 0.001$), determined using NAYA in water as a standard, is in agreement with the value ($\phi_F = 0.014$) previously determined by Cowgill (18). Compared to NAYA ($\phi_F = 0.049$), the quantum yield of RNase A indicates that some of the tyrosine residues in RNase A are quenched.

Studies carried out by Wills and Szabo (19) demonstrated that the fluorescence of Tyr is quenched in the presence of hydrogen-bond acceptors such as acetate. We have made a

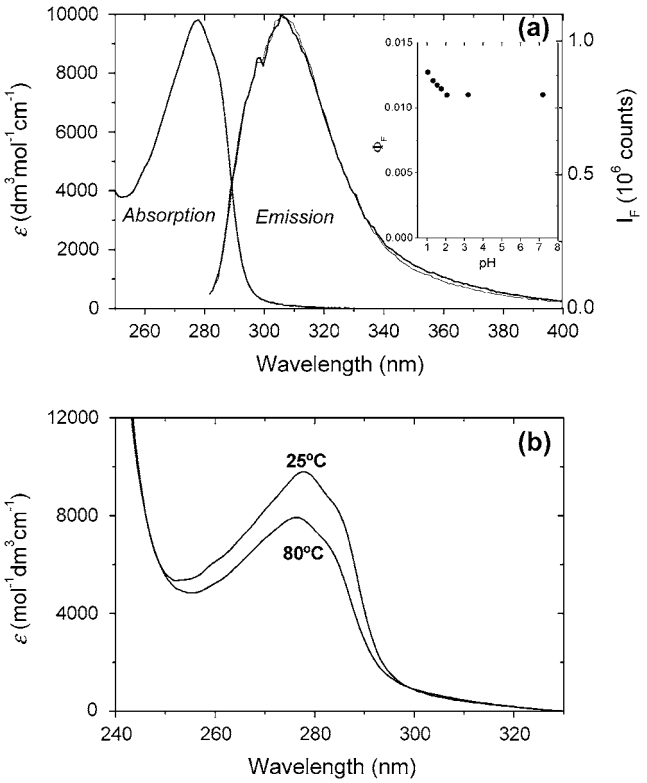

FIGURE 1 (*a*) Absorption ($\lambda_{abs}^{max} = 278$nm) and emission ($\lambda_{fluo}^{max} = 306$nm) spectra of RNase A in 10 mM sodium phosphate, pH 7.2, at 23°C. The emission spectra of RNase A at pH 2.2 (*darker line*) at 23°C show no change in the fluorescence intensity from pH 7 to pH 2.2. (*Inset*) Fluorescence quantum yield of RNase A in phosphate buffer at 23°C from pH 7.2 to pH 1. (*b*) Absorption spectra of RNase A at 25 and 80°C show a 2.5-nm blue shift and reduction in molar absorption coefficient (ε) at 80°C due to exposure to water.

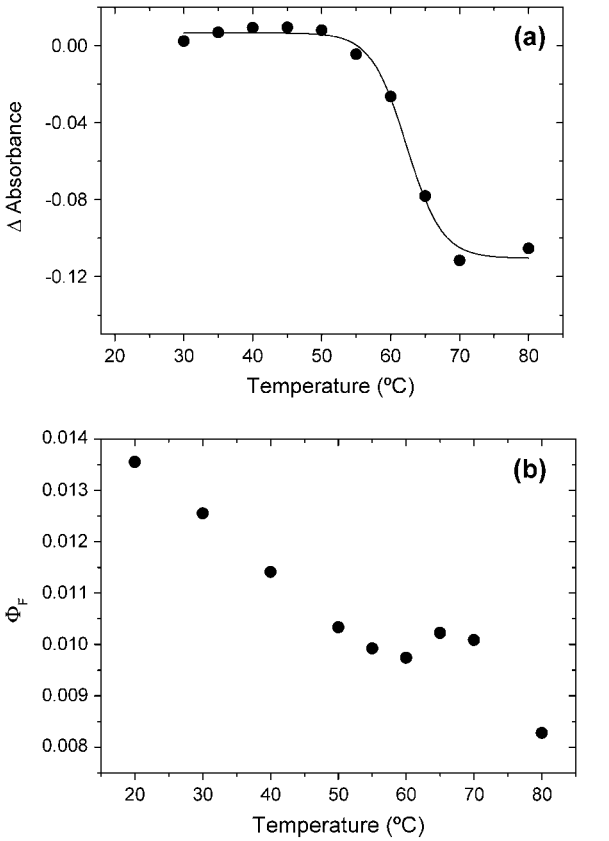

FIGURE 2 (*a*) Variation of differential absorbance (ΔA) of RNase A measured at $\lambda = 287$ nm with increasing temperature. (*b*) Fluorescence quantum yield (ϕ_F) of RNase A at pH 7 in 10 mM phosphate buffer as a function of increasing temperature.

similar observation for Tyr in UBQ, whose fluorescence is quenched as a result of proton transfer to a nearby carboxylate group of Glu-51 (5). Since previous studies have suggested that, at pH 5, Tyr-25 of RNase A is hydrogen-bonded to the carboxylate of Asp-14 (7,20), we have analyzed the fluorescence response to the pH change. Upon acidification to pH 2.2, there is no visible change in the fluorescence spectra and intensity relative to pH 7.2 (Fig. 1 *a*).

Temperature effects on the absorption and fluorescence spectra

At 80°C, the absorption spectrum of RNase A shows a decrease in the molar absorption coefficient and a blue shift of 1 nm, indicating the exposure of buried tyrosine residues (Fig. 1 *b*). Fig. 2 *a* shows a plot of the differential absorbance (ΔA) of RNase A measured at $\lambda = 287$ nm and pH 7.2 as a function of temperature (T). From the decrease in the absorbance in the 50–70°C temperature range, a melting temperature of $T_m = 62$°C was estimated.

In contrast to the typical sigmoidal curve observed in the case of ΔA vs. T, the fluorescence quantum yield decreases with temperature from $\phi_F = 0.013$ at 23°C to $\phi_F = 0.010$ at 60°C, then increases 4.6% from 60 to 65°C and finally decreases from 70 to 80°C (Fig. 2 *b*). Gally and Edelman (21) observed a similar dependence of the fluorescence quantum yield of RNase A on temperature, from which a value of $T_m = 58$°C was determined.

Denaturant effects on the absorption and fluorescence spectra

Similar to the effect of increasing temperature, the absorption spectra of RNase A show a 7% decrease in the molar extinction coefficient (ε) with increasing concentrations of added GuHCl and a 2-nm blue shift from $\lambda = 278$ nm in the absence of GuHCl to $\lambda = 276$ nm at 4.2 M GuHCl, indicating the exposure of buried tyrosine residues. At the same time, the fluorescence quantum yield increases from $\phi_F = 0.013$ at 0 M GuHCl to $\phi_F = 0.039$ at 4.2 M GuHCl, indicating a decrease in the efficiency of the fluorescence quenching.

Time-resolved fluorescence of RNase A

The fluorescence decays of RNase A in 10 mM phosphate buffer at pH 7 (23°C), measured with excitation at $\lambda_{exc} = 275$ nm and

emission at $\lambda_{em} = 295$ nm, can be fitted with a sum of three exponentials, providing decay times of $\tau_1 = 1.72 \pm 0.02$ ns, $\tau_2 = 180 \pm 15$ ps, and $\tau_3 = 30 \pm 8$ ps (Fig. 3). The errors represent the maximum variation in the values of the decay times obtained from five fluorescence decays measured with different samples and two emission wavelengths.

The fluorescence quantum yield, $\phi_F = 0.012 \pm 0.002$, calculated from the normalized fluorescence decay (using the decay times τ_i and preexponential coefficients A_i) and the value of the radiative rate constant of NAYA (9) of $k_f = 3.6 \times 10^7\ s^{-1}$ (Eq. 1), is similar to the experimental value, indicating that the fluorescence decay contains information on all the tyrosine residues, i.e., all fast decays were detected.

$$\phi_f = k_f \int_0^\infty I(t)dt = k_f \sum_{i=1}^{3} A_i \tau_i, \qquad (1)$$

with

$$\sum_{i=1}^{3} A_i = 1.$$

Since the fluorescence decays of NAYA are single exponential in low dielectric constant solvents (e.g., mixtures of dioxane:water below 70% v/v water concentration) (9), the fluorescence decay of a protein with six tyrosine residues in different environments could potentially be expected to display up to six different decay times (τ_i). The respective preexponential coefficients (A_i) would then be proportional to the concentration of each tyrosine residue, given that each decay time can be properly resolved (1,2) (see Discussion). In this case, we observe only three lifetimes and normalization of the preexponential coefficients for the six tyrosine residues present ($\sum_{i=1}^{3} A_i = 6$) provides a relative ratio of 0.9:1.0:4.1 for the three decay times. The result indicates that four tyrosines are strongly quenched ($\tau_3 = 30$ ps), one partially quenched ($\tau_2 = 180$ ps), and the sixth only slightly quenched ($\tau_1 = 1.72$ ns). Excitation of RNase A at different wavelengths gave similar results, except when the emission was collected at wavelengths longer than 305 nm. At these wavelengths, a residual 3.5-ns component, clearly due to an impurity, has been detected.

In summary, the foregoing results show that the fluorescence decays of RNase A can be described as triple exponentials and that the preexponential coefficients indicate that four tyrosines have a very short decay time (30–40 ps), a fifth tyrosine a relatively short decay time (165–195 ps), and the last a relatively long lifetime (1.70–1.74 ns).

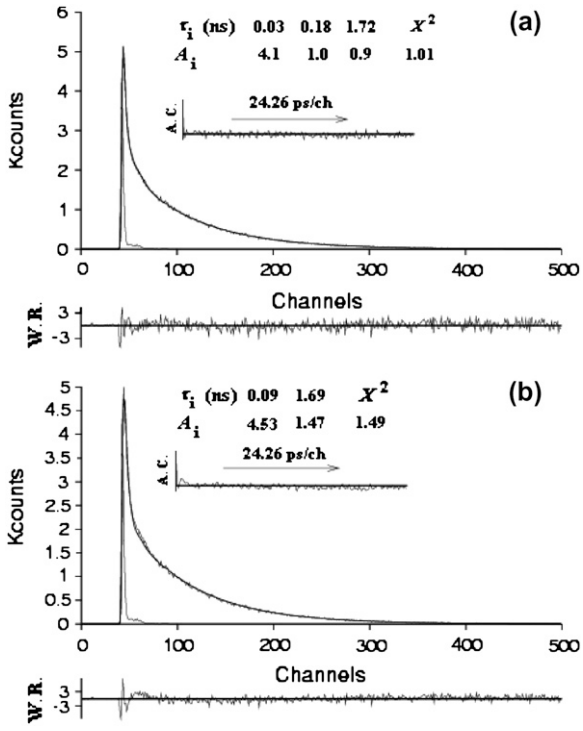

FIGURE 3 Fluorescence decay of RNase A in 10 mM phosphate buffer at pH 7 and at 23°C with a timescale of 24.26 ps/channel is best fit with a sum of three exponentials (*a*) with decay times $\tau_1 = 1.72$ ns, $\tau_2 = 180$ ps, and $\tau_3 = 30$ ps as seen from the autocorrelation (*A.C.*), weighted residuals (*W.R.*), and χ^2 of 1.01. On normalization of the ratios of preexponential coefficients, a distribution of ~1:1:4 is observed. (*b*) Fluorescence decay of RNase A in 10 mM phosphate buffer at pH 7 and at 23°C with a timescale of 24.26 ps/channel fit with a sum of two exponentials, $\chi^2 = 1.49$ with decay times $\tau_1 = 1.69$ ns and $\tau_2 = 90$ ps and preexponential coefficients of $A_1 = 1.47$ and $A_2 = 4.53$.

Temperature and denaturant effects on the time-resolved fluorescence of RNase A

The fluorescence decays of RNase A remain triple exponential up to 80°C. The decay times (τ_i) and preexponential coefficients (A_i) are plotted in Fig. 4, *a* and *b*, as a function of temperature.

The longest decay time τ_1 gradually decreases from 1.7 to 1.5 ns at 50°C and falls sharply from 1.5 to 0.88 ns at 70°C, indicating a transition in the region from 50 to 70°C. τ_2 increases from 180 ps at 23°C to 400 ps at 64°C and then decreases slightly to 380 ps at 70°C, whereas τ_3 increases from 30 ps at 23°C to 80 ps at 70°C (Fig. 4 *a*). The increase of τ_2 and τ_3 indicate that five tyrosine residues are less quenched in the unfolded state.

Significantly, the preexponential coefficients show an alteration in the relative ratios from ~1:1:4 at 23°C to ~1:3:2 at 70°C. This indicates that two of the four strongly quenched tyrosines become only partially quenched when the protein unfolds (Fig. 4 *b*).

The chemical unfolding of RNase A employing GuHCl was also followed using time-resolved fluorescence. From 0 to 4.2 M GuHCl, the long decay time τ_1 increases slightly from 1.71 to 1.86 ns, τ_2 increases from 165 to 754 ps, and τ_3 increases from 34 to 104 ps (Fig. 5 *a*). The preexponential coefficient A_1 increases from 1 to 1.3, A_2 from 1 to 2.7, and A_3 remains approximately constant at 4 up to 2.6 M GuHCl, and sharply decreases to 2 in the 2.6–4.2 M GuHCl concentration range (Fig. 5 *b*). As in the case of thermal

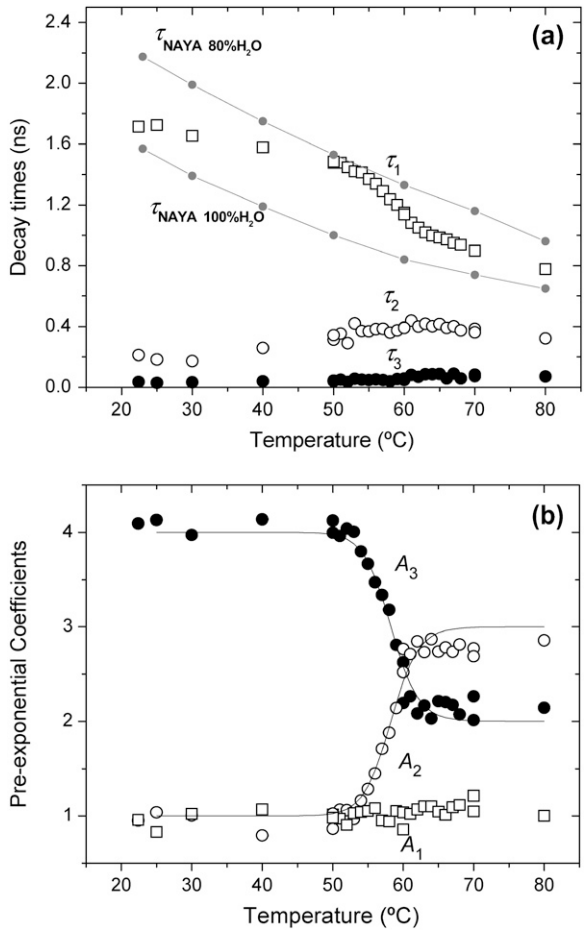

FIGURE 4 (*a*) The longest decay time of RNase A τ_1 (*squares*) decreases from 1.72 to 0.82 ns, τ_2 (*open circles*) increases from 180 to ~400 ps, whereas τ_3 (*solid circles*) increases from 30 to ~80 ps from 23 to 80°C. The values of τ_1 fall in between the decay times of NAYA in mixtures of 20:80 dioxane/water and neat water (*solid circles* and *solid lines*). (*b*) The normalized preexponential coefficient A_1 (*squares*) is constant within experimental error, A_2 (*open circles*) increases from 1 to ~3 and A_3 (*solid circles*) decreases from 4 to 2 from 23 to 80°C. Solid lines shown are theoretical fits assuming the six-Tyr model (Eq. 13), from which values of $\Delta H =$ 461.4kJ/mol and $\Delta S = 1.392$ kJ/mol/K were calculated.

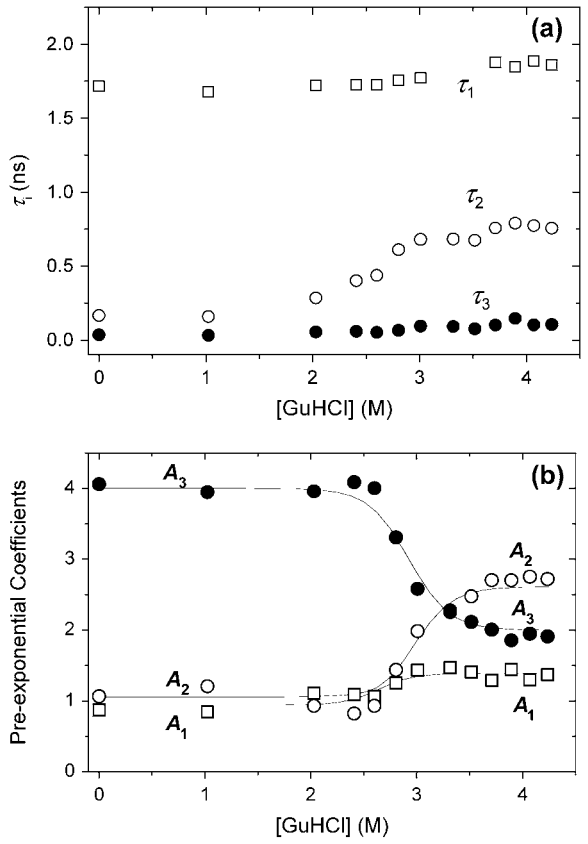

FIGURE 5 (*a*) Upon increasing the concentration of GuHCl from 0 to 4.2 M, τ_1 (*squares*) increases from 1.71 to 1.85 ns, τ_2 (*open circles*) increases from 160 to 755 ps, and τ_3 (*solid circles*) increases from 33 to 104 ps. (*b*) The normalized preexponential coefficient A_1 (*squares*) increases from 0.9 to 1.3, A_2 (*open circles*) increases from 1 to 2.7, and A_3 (*solid circles*) decreases from 4 to 2 from 0 to 4.2 M GuHCl. The continuous line for A_1 is a fit using a sigmoidal function; the solid lines shown for A_2 and A_3 are theoretical fits assuming the six-Tyr model from which values of $\Delta G^{23°C}_{H_2O} =$ 37.8kJ/mol/K and $m = 12.9$ kJ/mol/M were determined.

unfolding, chemical unfolding of RNase A induces a change in the environment of two highly quenched tyrosine residues in the native state, which become partially quenched in the unfolded state.

DISCUSSION

Assignment of the decay components to the corresponding tyrosine residues

Fluorescence decays of RNase A

The fluorescence decay of native RNase A, $I_N(t)$ is the sum of the fluorescence decays of the six individual tyrosines $I_i(t)$. Theoretically, if each tyrosine displayed a single exponential decay, $I_N(t)$ would be given by Eq. 2, where τ_i is the fluorescence decay time and A_i the preexponential coefficient of each tyrosine (Y_i) residue.

$$I_N(t) = \sum_{i=1}^{6} I_i(t) = \sum_{i=1}^{6} A_i e^{(-t/\tau_i)}. \quad (2)$$

The preexponential coefficients represent the fluorescence intensity of each tyrosine residue at $t = 0$, and can be used to evaluate the mol fraction of the residue in the excited and ground states after appropriate corrections (4). Briefly, the fluorescence intensity of each tyrosine residue at $t = 0$, $I_i(0)$, is equal to the concentration of the corresponding excited species $[Y_i^*](0)$ multiplied by its radiative rate constant $k_{fi}(I_i(0) = k_{fi} \times [Y_i^*](0))$. For a decay measured at a given emission wavelength, λ_{em}, the respective preexponential coefficient A_i is equal to the fluorescence intensity of the residue $(k_{fi} \times [Y_i^*](0))$ times the fraction of the emission, $f_i(\lambda_{em})$, that is detected at λ_{em}, modulated by an instrumental constant, c_{inst} (Eq. 3).

$$A_i = c_{inst} \times f_i(\lambda_{em}) \times k_{fi} \times \left[Y_i^*\right](0), \quad (3)$$

with:

$$f_i(\lambda_{em}) = \frac{I_i(\lambda_{em})}{\int I_i(\lambda) d\lambda}, \quad (4)$$

where $\int I_i(\lambda) d\lambda$ is the total fluorescence emission.

Thus, Eq. 3 permits determination of the excited-state mol fractions of the residues when the k_{fi} and $f_i(\lambda_{em})$ are known. The radiative rate constant of NAYA does not change from dioxane ($3.5 \times 10^7\ s^{-1}$) to water ($3.6 \times 10^7\ s^{-1}$); hence, k_{fi} of each tyrosine residue is expected to have similar values. Also, the emission spectra of NAYA in dioxane and water show only a very small bathochromic shift (~2 nm) and, as such, the normalized spectra are almost coincident. Consequently, the *f*i of each tyrosine residue can be considered to be the same. Thus, the preexponential coefficients (A_i) are proportional to the excited state concentrations at $t = 0$ without further correction.

The ground-state concentrations of the tyrosine residues are proportional to the excited-state concentrations at $t = 0$ divided by their respective molar extinction coefficients (ε_i) at the excitation wavelength. In the case of NAYA, an ~20% change in ε_{max} is observed upon going from dioxane to water. However, an isosbestic wavelength exists at $\lambda = 265$ nm (9). As a result, despite the fact that the six tyrosine residues are located in different regions of the protein, with selective excitation at $\lambda_{exc} = 265$ nm, all the tyrosine residues have the same molar extinction coefficient and absorb the same fraction of the incident excitation intensity. In conclusion, the preexponential coefficients obtained from the fluorescence decays of RNase A with excitation at $\lambda = 265$ nm, are directly proportional to the ground-state concentration of each tyrosine residue with no correction required for the fraction of light emitted ($f_i(\lambda_{em})$), radiative rate constant (k_f), or molar extinction coefficient.

In the case of native RNase A, the fluorescence decay is best fit with a sum of three exponential functions. Therefore, the 1:1:4 ratio of the normalized preexponential coefficients ($\sum_{i=1}^{3} A_i = 6$) implies that four tyrosine residues are strongly quenched and one partially quenched, whereas the third exhibits a decay time close to that of NAYA in water (slightly quenched). However, the foregoing interpretation relies on the assumption that all tyrosine residues possess single exponential decays.

The fluorescence decay of NAYA in dioxane-water mixtures exhibits single exponential decays over a wide temperature range below 70% water content. Above this water content, a second shorter decay time (~400 ps) starts to develop and its normalized preexponential ultimately reaches the value of 0.12 in water (9). Very similar observations were made with the single-tyrosine protein UBQ, but the preexponential value was greater (5). The observation of this double-exponential decay, which results from electron transfer from one of the three cresol rotamers to the protein backbone, depends on three factors: i), the relative mol fractions of the ground-state rotamer population, the rotamer conformations being determined by rotation about the C_α-C_β bond (α); ii), the rotational rate constants for interconversion between the rotamers, k_r and k_r'; and iii), the photo-induced electron transfer rate constant, k_{ET}, which depends strongly on solvent polarity (9). In dioxane/water mixtures below 70% water, the decays are single exponentials because k_{ET} is too small.

The structure of RNase A obtained by x-ray crystallography or by NMR (22) indicates that three tyrosines (Tyr-25, Tyr-73, and Tyr-97) are buried in the interior of the protein, two (Tyr-92 and Tyr-115) are ~50% exposed and one (Tyr-76) is 70–80% exposed. Therefore, it is quite reasonable to assume that at least five of the tyrosines will exhibit single-exponential decay at 23°C. Although the sixth or most-exposed tyrosine might potentially show double exponential decay, the fact that the preexponential coefficient of the longest decay time, assigned to this most exposed tyrosine (see below), is approximately equal to unity over the entire temperature range studied demonstrates that all of the tyrosines undergo single-exponential decay. This fact also implies that the mol fraction of rotamers α undergoing electron transfer to the backbone is low.

Mechanisms of fluorescence quenching

When electron transfer to the protein backbone would be the sole mechanism of fluorescence quenching, the decay of RNase A at 23°C would be expected to be described by a sum of three exponentials with decay times of $\tau_1 \cong 5$ ns, corresponding to three tyrosine residues buried in the interior of the protein, a second decay time $\tau_2 \cong 4$ ns corresponding to the 50% exposed tyrosines, and a third decay time (τ_3) corresponding to the decay time of NAYA in 70–80% water/dioxane ($\tau_3 \cong 2$ ns). The much shorter decay times observed in the fluorescence decay of RNase A at 23°C clearly show that at least five of the tyrosine residues are highly quenched. Specifically, the shortest decay time of RNase A (τ_3) indicates that four tyrosines suffer an ~150-fold reduction in fluorescence intensity ($\tau_0/\tau_3 = 5/0.03$) as a result of quenching.

In the presence of quenching, the reciprocal fluorescence decay time of each individual tyrosine residue (τ_i) is equal to the sum of the radiative (k_{fi}), the radiationless (k_{nri}), and the quenching (k_{qi}) rate constants, which leads to Eq. 5, where τ_{0i} represents the unquenched lifetime of each Tyr residue, assumed equal to the lifetime of NAYA in the appropriate dioxane/water mixture (9)

$$k_{qi} = \frac{1}{\tau_i} - \frac{1}{\tau_{0i}}. \quad (5)$$

From this equation, values of $k_{q1} = 7 \times 10^7\ s^{-1}$, $k_{q2} = 5.3 \times 10^9\ s^{-1}$, and $k_{q3} = 3.0 \times 10^{10}\ s^{-1}$ are obtained for the pseudounimolecular quenching rate constants of the three groups (1:1:4) of tyrosines, respectively.

Quenching by proton transfer

Among the fluorescence quenching mechanisms known for tyrosine within proteins, quenching by proton transfer to a carboxylate of an aspartic or glutamic amino acid residue has been observed in bovine ubiquitin (5). Studies have suggested that Tyr-25 is hydrogen bonded to Asp-14. As a result, quenching of this tyrosine could occur as a result of excited-state proton transfer (ESPT). To check if ESPT might be responsible for tyrosine fluorescence quenching in RNase A, the fluorescence quantum yield was measured as a function of pH from pH 7 to pH 1 at 23°C (Fig. 1 *a*, *inset*). Because ESPT does not occur from tyrosine to protonated carboxylate groups, a substantial increase in the fluorescence yield of RNase A would be expected at sufficiently low pH values if ESPT were the mechanism responsible for fluorescence quenching. The fluorescence quantum yield showed no change between pH 7 and pH 2 and only a 20% increase in fluorescence intensity below pH 2. Previous studies have shown that, at pH 2, RNase A has a $T_m = 30°C$ (23). The lack of a change in fluorescence intensity in the pH range from 7 to 2 (Fig. 1 *a*, *inset*) indicates that, even though Tyr-25 may be hydrogen bonded to Asp-14, the quenching of Tyr-25 does not result from proton transfer to nearby carboxylate groups. The modest increase in fluorescence intensity below pH 2 at 25°C is attributed to the pH-induced denaturation of RNase A, as previously stated by Cowgill (24).

Quenching by disulfide bridges

Three decades ago, Cowgill classified the fluorescence of the tyrosine residues in RNase A in the following manner: Tyr-25, Tyr-97, and Tyr-92 as being buried in the interior, hydrogen bonded to carbonyl groups, and completely quenched, whereas Tyr-73, Tyr-76, and Tyr-115 are partially quenched by different mechanisms varying from quenching by the hydrated peptide carbonyl group, by disulphide bonds, and by resonance energy transfer to other quenched tyrosines (25). However, the x-ray crystal structure of the protein shows that Tyr-92 is neither completely buried nor hydrogen bonded to a carbonyl group. Hence, the quenching of this tyrosine residue cannot be described by the mechanism proposed by Cowgill. In an era when time-resolved fluorescence spectroscopy and crystal structure analyses were in their initial stages, his work on this protein remains noteworthy. However, the discrepancy observed for Tyr-92 suggests that the classification adopted for tyrosine residues in RNase A requires revision. In this context, Swadesh et al. subsequently proposed that the quenching of tyrosine in RNase A is a result of complex formation between tyrosine residues and disulphide bridges (26).

Mechanism of quenching by disulfide bridges

Different mechanisms of fluorescence quenching of tyrosine or tryptophan residues by disulphide bridges have been proposed, including excited-state electron transfer (27), energy transfer (28), and short-range interactions that permit vibrational dissipation of the excitation energy (29,30).

The standard Gibbs energy of electron transfer ΔG^0_{ET} from tyrosine to a disulphide bridge can be estimated from the difference between the oxidation potential of cresol ($E^{ox}_D = 1.4$V versus saturated calomel electrode in acetonitrile) (31) and the reduction potential of cystine ($E^{red}_A = -0.33$V versus saturated calomel electrode in water) (32) given by Eq. 6, assuming that cresol and cystine are representative models for the donor (tyrosine ring) and acceptor (disulphide bridge), respectively. On the basis of these values it is clear that disulfides are excellent electron acceptors and that the excited-state electron transfer from tyrosine to disulfide bridges is strongly exergonic ($\Delta G^0_{ET} = -2.6$eV from Eq. 6).

$$\Delta G^{0}_{ET} = E^{ox}_D - E^{red}_A - h\nu + \Delta G^0(\varepsilon). \tag{6}$$

In Eq. 6, the excitation energy ($h\nu = 4.32$ eV) was taken from the mid-energy value of the absorption and emission spectra of NAYA in dioxane-water mixtures. $\Delta G^0(\varepsilon)$ (Eq. 7) accounts for the Coulombic interaction of the ion pair (ΔG_{ionic}) and corrects the $E^{ox}_D - E^{red}_A$ values for transfer from acetonitrile to water ($\Delta\Delta G_{solv}$), in Joule, (33).

$$\begin{aligned}\Delta G^0(\varepsilon) &= \Delta G_{ionic} \\ &= -\frac{e^2}{4\pi\varepsilon_0\varepsilon_{solv}(r_{A^-} + r_{D^+})} \\ &\quad - \frac{e^2}{8\pi\varepsilon_0}\left(r^{-1}_{A^-} + r^{-1}_{D^+}\right)\left(\varepsilon^{-1}_{solv} - \varepsilon^{-1}_{ref}\right).\end{aligned} \tag{7}$$

However, the experimental reduction potential of cystine refers to a two-electron, two-proton irreversible reaction and not a single electron transfer as is in the case of the excited-state electron transfer from tyrosine to disulphide bridges in RNase A. Consequently, we also evaluated ΔG^0_{ET} by using the experimental ionization potential of cresol ($IP = 8.33$ eV) and experimental electron affinities of model compounds (dimethyl disulfide, $EA = 1.87$ eV (34) or diethyl disulfide, $EA = 1.95$ eV (35) (Eq. 8)).

$$\Delta G^0_{ET} = IP - EA - h\nu + \Delta G^0(\varepsilon). \tag{8}$$

Once again, the values of ΔG^0_{ET} (e.g., for dimethyl disulfide) indicate that disulfides are excellent electron acceptors and that the excited-state electron transfer from tyrosine to disulfide bridges is strongly exergonic ($\Delta G^0_{ET} = -1.9$ eV from Eq. 8). In the case of Eq. 8, $\Delta\Delta G_{solv}$ corrects the *IP-EA* values from gas phase to water (i.e., $\varepsilon_{ref} = 1$ in Eq. 7).

The values of ΔG^0_{ET} suggest that excited-state electron transfer in the tyrosine-disulfide bridge should be practically activationless. In fact, although the value of ΔG^0_{ET} may lie in the Marcus inverted region ($\Delta G^0_{ET} < -\lambda$ in Eq. 9) (36,37) when a value $\lambda \approx 1.6$ eV is assumed for the reorganization energy (38), it is well known that Eq. 9 (Marcus' classic theory) overestimates the increase in the Gibbs activation energy of electron transfer $\Delta G^{\#}_{ET}$ with decreasing ΔG^0_{ET} in the inverted energy region (39).

$$\Delta G_{ET}^{\#} = \frac{\left(\Delta G_{ET}^{0} + \lambda\right)^2}{4\lambda}. \quad (9)$$

The absence of a temperature dependence of the two shortest decay times of RNase A in the pretransition temperature range (23–50°C) also indicates a practically activationless quenching of the corresponding five tyrosines. Hence, the electron transfer rate constant (k_{ET}) from tyrosine to a nearby disulfide bridge should depend essentially on the effective donor-acceptor distance R (Eq. 10).

$$k_{ET} = k_0 \exp(-2(R - R_0)/L).\exp(-\Delta G_{ET}^{\#}/k_B T). \quad (10)$$

In Eq. 10, R is the center-to-center distance, R_0 is the sum of the van der Waals radii of the acceptor and donor, L is the orbital overlap parameter, and k_0 is the preexponential coefficient, given by Eq. 11, where $J_0(R_0)$ is the coupling matrix element at the contact distance R_0.

$$k_0 = \frac{2\pi}{\hbar}(4\pi\lambda k_B T)^{-1/2} \times J_0(R_0)^2. \quad (11)$$

The center-to-center distances from the six tyrosines of RNase A to the closest disulfide bridge, obtained from the x-ray crystal structure (Table 1) and MD simulations at 23°C (Fig. 6), show that four tyrosines (25, 73, 92, and 97) are within 5–6 Å, Tyr-115 is at ~7 Å and Tyr-76 at ~12 Å. Clearly, then, electron transfer will be the dominant deactivation process for the first five tyrosines.

This assignment is in agreement with results obtained with four mutants of Rnase A (Y73W, Y76W, Y92W, and Y115W) by Navon et al. (8), in which Tyr-73, Tyr-76, Tyr-92, and Tyr-115 were replaced one by one with a tryptophan. Since tryptophan is an equally good electron donor as tyrosine (IP = 7.54 eV (40); $h\nu$ = 4.12 eV for 3-methylindole), the four tryptophans should be as quenched as the corresponding assigned tyrosines in the unaltered protein. In fact, the tryptophan in Y76W is practically not quenched, in Y73W and Y92W the tryptophan is strongly quenched, and in Y115W it is also quenched but to a lesser extent than in the two former. However, since the value of T_m of the Y92W mutant (~61°C from UV spectroscopy) was found substantially larger than those of the remaining three mutants (all within 53 ± 1°C), it seems that at least one mutation has induced significant conformational changes with respect to the wild-type protein. Therefore, despite the agreement of Navon's data with our assignment, their results cannot be taken as a clean proof of this assignment.

TABLE 1 Solvent accessibility (SA) and distances (R) of tyrosines (TYR) to the nearest disulfide bridge (CYS), calculated from the center of the tyrosine ring to the center of the disulfide bond using the x-ray crystal structure

TYR	SA (% H_2O)	CYS	R (23°C) Å	R (87°C) Å
25	10–20	26–84	5.36 ± 0.46*	7.49 ± 0.36
73	10–20	58–110	5.36 ± 0.60	5.34 ± 0.45
76	70–80	58–110	12.8 ± 0.69	12.9 ± 0.80
92	50–60	40–95	5.41 ± 0.60	6.23 ± 0.47
97	0–10	40–95	5.96 ± 0.39	5.31 ± 0.43
115	50–60	58–110	6.98 ± 0.86	6.88 ± 1.15

The average distances were calculated from simulations carried out at 23 and at 87°C (averages taken over the last 2 ns of the simulation).
*Tyr-25 also showed an R distance of 6.5 ± 0.54 Å for periods >3.5 ns.

Under the assumption that $\Delta G_{ET}^{\#}$ is close to zero or simply identical for all tyrosines, the electron-transfer rate constant will depend on three parameters k_0, L, and R (Eq. 10). A plot of ln k_{ET} vs. R should therefore be linear. Strictly, the experimental kET represents an average kET and not its value at the average R. However, the maximum variation in R for all tyrosines is around 0.3 Å except for Tyr-92, which shows variations up to 0.8 Å. Studies on electron transfer in proteins between redox centers have shown that kET is significantly modulated by the intervening medium (42) where kET is faster between covalently bonded redox centers than through vacuum. On a closer look at the crystal structure, all tyrosines seem equivalent with respect to their medium except for Tyr-115, which has the –CH2– group of one of the cysteines in between the tyrosine ring and the center of the disulphide bridge Cys-58–Cys-110. However, no covalent bond is apparent directly between the tyrosine rings and disulphide bridges from the crystal structure. A logarithmic plot of the k_{ET} values for the three groups of tyrosine in RNase A versus the tyrosine-disulfide distances provides estimates of the parameters of Eq. 10 of $k_0 = 2.4 \times 10^{12}$ s^{-1} and L = 2.45 Å. These values are consistent with values of these parameters reported for other electron-transfer pairs (42,43).

Reconstruction of fluorescence decays

Employing the values of k_0 and L, we calculated values of the fluorescence decay times $\tau_i(R_i)$ of the six tyrosines and used these to construct a theoretical hexa-exponential decay of RNase A with 38,000 counts at the peak channel. The theoretical fluorescence decay was convoluted with the experimental pulse and then analyzed using sums of two and three exponentials. A sum of three exponentials was found to be sufficient to fit the theoretical hexa-exponential decay (Fig. 7). Thus, the decay times of four of the tyrosines are close enough to each other to be experimentally indistinguishable and appear as a single decay time (τ_3) with a fourfold larger preexponential coefficient A_3. The decay times of Tyr-115 (τ_2) and Tyr-76 (τ_1) are sufficiently different to require another two exponential terms in the fit. The recovered decay times and respective preexponentials of τ_1 =1.75 ns (A_1 = 1.05) τ_2 =127 ps (A_2 = 0.93) τ_3 = 40 ps (A_3 = 4.02) are similar to those obtained from experimental decays.

Thermal and chemical unfolding of RNase A by TRFS

On the basis of the above assignment, the thermally or chemically induced changes occurring in different regions of the protein where the tyrosine residues are located can now

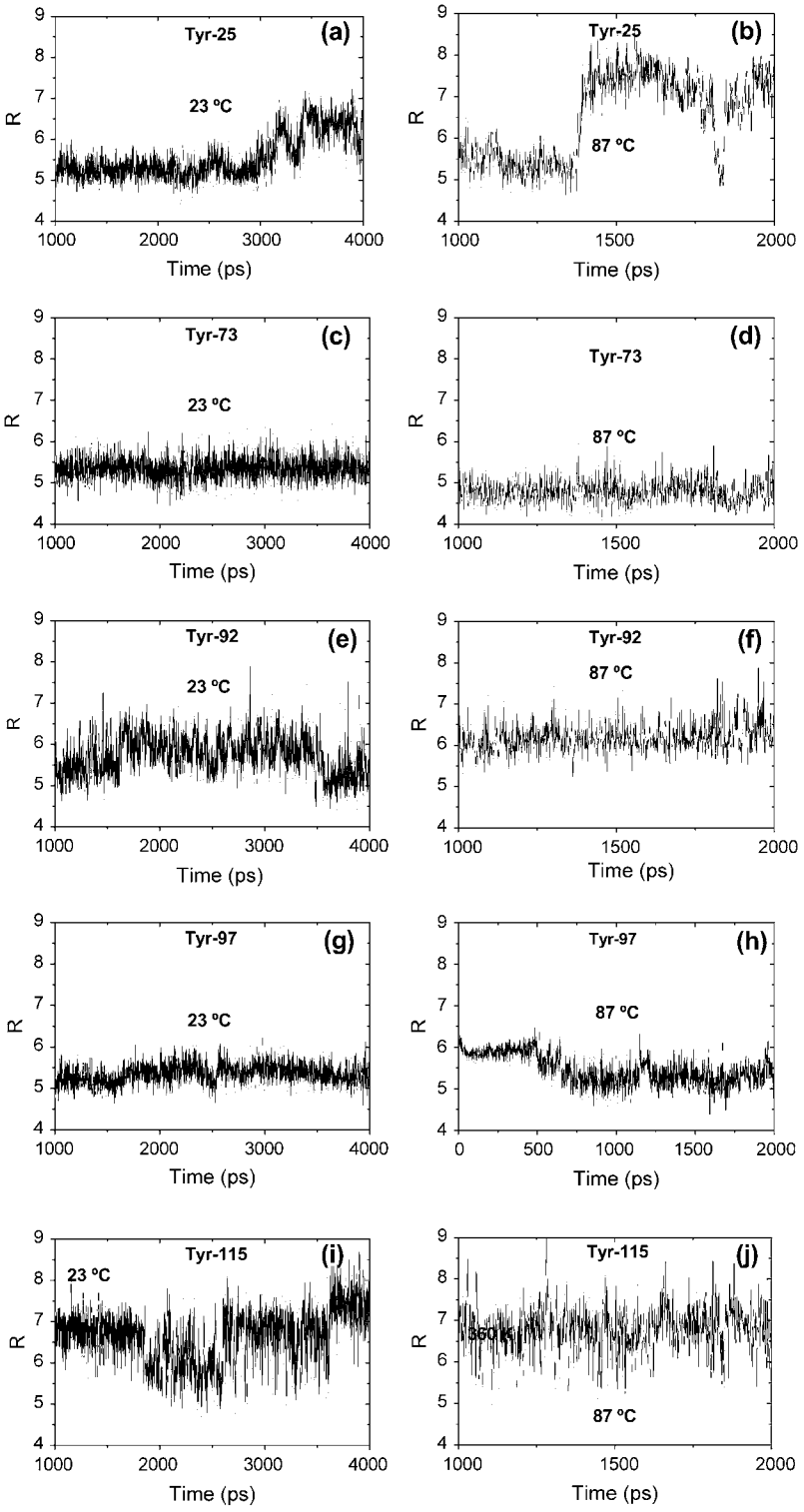

FIGURE 6 Comparison of the distances from the center of the tyrosine ring to the center of the disulfide bridge (R) for (*a*) Tyr-25 from disulfide bridge C26–C84 at 23°C and (*b*) at 87°C, (*c*) Tyr-73 from C58–C110 at 23°C and (*d*) at 87°C, (*e*) Tyr-92 from C40–C95 at 23°C and (*f*) at 87°C, (*g*) Tyr-97 from C40–C95 at 23°C and (*h*) at 87°C, and (*i*) Tyr-115 from C58–C110 at 23°C and (*j*) at 87°C.

be followed by monitoring the respective decay times and preexponential coefficients.

Thermal unfolding

The study of the parent compound NAYA in water as a function of temperature showed a gradual decrease in the decay times with increasing temperature (Fig. 4 *a*). In the case of RNase A, τ_1 decreased gradually from 20 to 50°C, and sharply from 50 to 60°C, whereas its preexponential coefficient remains constant. The sharper decrease in τ_1 reflects the exposure of the slightly buried Tyr-76 to water upon denaturation. This decrease results from the fact that the

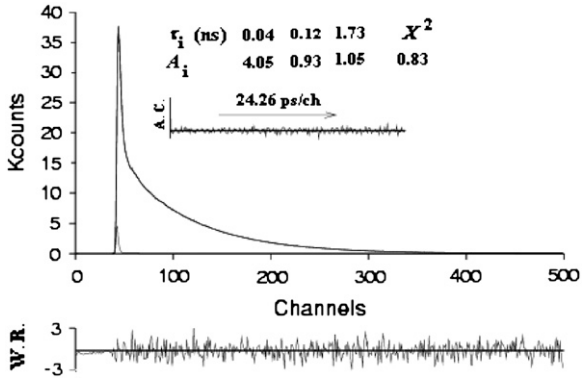

FIGURE 7 Analysis of a theoretical hexa-exponential fluorescence decay of RNase A with 38,000 counts at the maximum. The six decay times were calculated with Eqs. 5 and 10 using values of $k_0 = 2.4 \times 10^{12}\ s^{-1}$ and $L = 2.45$ Å and the distances of each tyrosine residue presented in Table 1 at 23°C. The decay can be fitted with a triple exponential with decay times and preexponentials of $\tau_1 = 1.75$ ns ($A_1 = 1.05$) $\tau_2 = 127$ ps ($A_2 = 0.93$) $\tau_3 = 40$ ps ($A_3 = 4.02$).

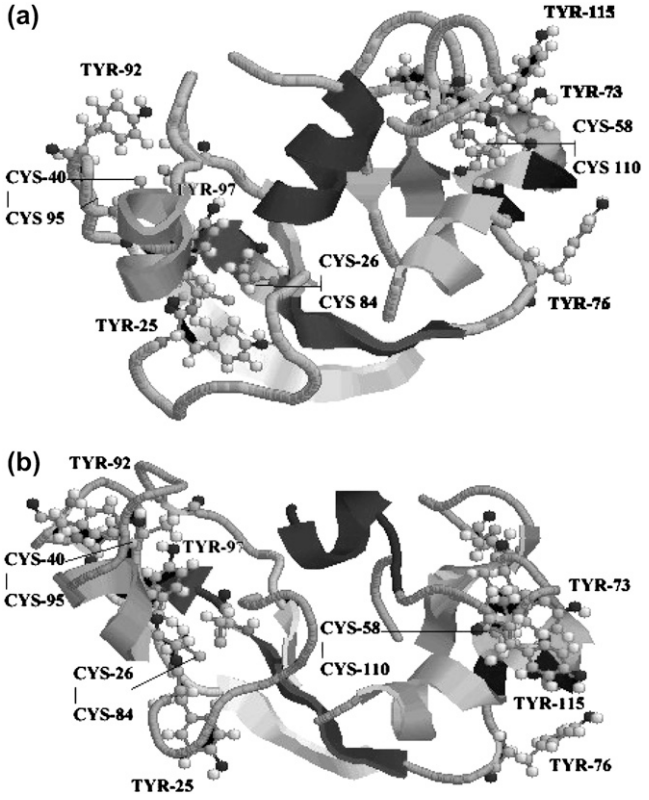

FIGURE 8 Stereoscopic views of one of the structures of RNase A from the simulations carried out at (*a*) 23°C and (*b*) 177°C.

decay time of the unfolded state (corresponding to Tyr-76 in ~95% water). Using the pre- and posttransitional baselines of τ_1, we calculated a $T_m = 59.2$°C. This value essentially reflects the response of the protein to heating in the region where Tyr-76 is located, which is on a loop between β-strand III and β-strand IV (Fig. 8 *a*). Additionally, in the temperature range from 20 to 50°C, we expect k_{ET} to remain constant or increase slightly with temperature. However, a plot of k_{ET}, calculated from $1/\tau_1 - 1/\tau_0$, where τ_0 is the decay time of NAYA in a mixture of 20:80 dioxane/water from 20 to 50°C, shows a reduction in k_{ET} with increasing temperature, which would only be possible if the distance (R) between the tyrosine residue and the nearest disulfide bridge increases with temperature. No increase in R is apparent from the MD simulations, which predict a constant value of $R \sim 12.8$ Å for Tyr-76 from 23 to 87°C (Table 1). The decrease in k_{ET} from 20 to 50°C suggests a pretransition, observed from the decay time τ_1 that is not adequately predicted by the MD simulations.

The decay times τ_2 and τ_3 remain almost constant, within experimental error, in the pretransition temperature region below 50°C. However, in contrast to the normal temperature dependence, τ_2 and τ_3 increase from 50 to 80°C. This tendency derives from a reduction in quenching, likely due to an increase in the distance (R) from the tyrosine rings to the quenchers (disulphide bridges) as a result of unfolding. In addition, A_2 goes from 1 to 2.8, while A_3 decreases from 4 to 2 in the temperature range from 50 to 80°C. The decrease of A_3 from 4 to 2 suggests that two of the tyrosines that are highly quenched at 23°C become only partially quenched at 80°C. On the basis of the tyrosine-disulfide distances obtained from the MD simulation at 87°C (Table 1), it seems likely that these two tyrosines are Tyr-25 and Tyr-92. Tyr-25 and Tyr-92 are located in different parts of the protein, Tyr-25 in α-helix II (residues 24–34) and Tyr-92 on a loop between β-strand IV and β-strand V (see Fig. 8 *a*).

Summarizing, Tyr-73 and Tyr-97 remain ~5.3 Å from the closest disulfide bridge and continue to be strongly quenched, whereas Tyr-25 and Tyr-92 increase their distance from the closest disulfide bridge from ~5.4 Å to 7.5 and 6.2 Å, respectively, and are only partially quenched upon denaturation. This suggests that the regions associated with Tyr-25, namely α-helix II, and with Tyr-92, in the loop in between β-strand IV and β-strand V, lose their structure partially or completely, whereas β-strand III (Tyr-73) and β-strand V (Tyr-97) maintain their structure even at 80°C.

Chemical unfolding

In the case of chemical unfolding, the temperature effect on the decay times is absent, leaving only the displacement of the tyrosine residues away from their disulphide bridges and exposure to water as the causes of changes in the decay times. Below 2 M GuHCl, there is no appreciable change in the decay times, whereas above this concentration there is an increase in all the decay times (τ_1 increases from ~1.70 to 1.87 ns, τ_2 from 0.16 to 0.76 ns, and τ_3 from ~30 to 100 ps), indicating a significant increase in some of the tyrosine-disulphide bridge distances (Fig. 5 *a*).

Previous studies have suggested that the denaturant-induced unfolded state of RNase A exhibits less conformational order than the thermally unfolded state. Thus, MD simulations were carried out at 177°C in an attempt to evaluate the distances from the tyrosine residues to their nearest disulphide bridge (R) in a more expanded unfolded state. Fig. 9 shows an increase in R for Tyr-76 during part of the simulation to 13.5 Å (compared to 12.8 Å at 23 and 87°C), which would correspond to $\tau_1 = 1.86$ ns.

As in the case of thermal unfolding, the preexponential coefficient of the four strongly quenched tyrosines (A_3) changes from ~4 in the absence of GuHCl to 2 at 4.2 M GuHCl, indicating that two tyrosines become less quenched upon unfolding. However, the final distribution of decay times 1.3:2.7:2 deviates significantly from the 1:3:2 distribution expected for the unfolded state of RNase A. This is essentially due to the increase from 1 to 1.3 of A_1 for the weakly quenched Tyr-76. These results suggest that, at 4.2 M GuHCl, one of the three partially quenched tyrosine residues may adopt in part R-values similar to those of Tyr-76. Fig. 9 shows that the distance of Tyr-92 to its nearest disulphide bridge increases up to ~12 Å and starts to fall again before the end (2 ns) of the simulation. This suggests that, in a more unfolded state of RNase A, Tyr-92 might temporarily adopt conformations with a long decay time similar to Tyr-76, leading to the observed increase in the preexponential associated with the long decay time (τ_1) to above unity.

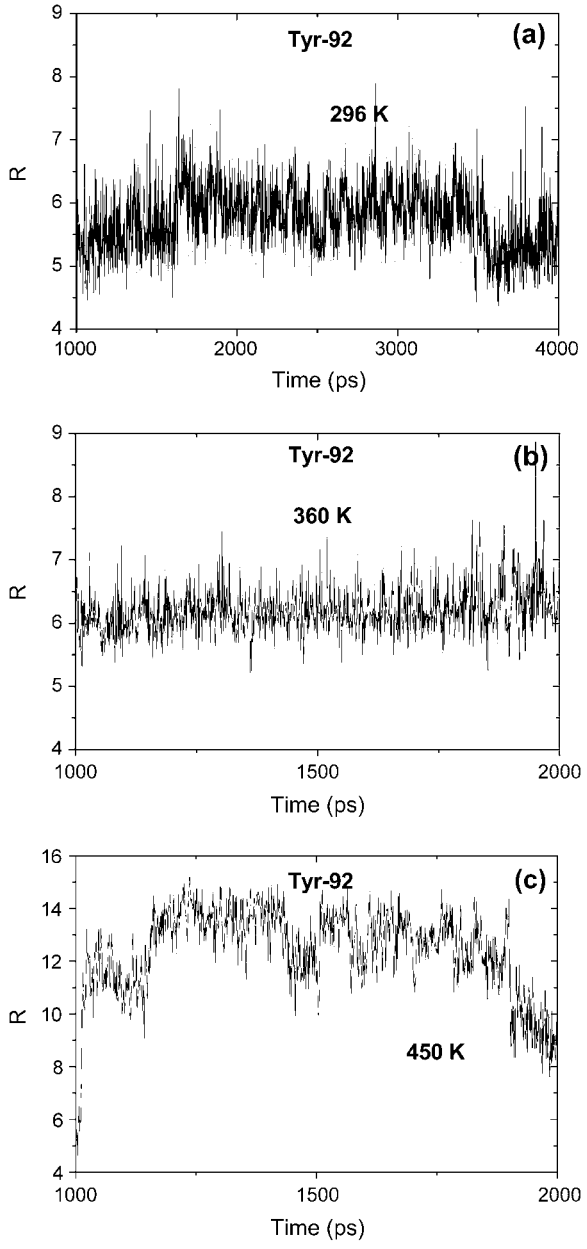

FIGURE 9 Distances from the center of the tyrosine ring to the center of the disulfide bridge (R) for (*a*) Tyr-92 from C40–C95 at 23°C, (*b*) 87°C, and (*c*) 177°C from molecular dynamics simulation started from the native state.

Thermodynamics of RNase A unfolding from preexponential coefficients

In a previous study on thermal unfolding of ubiquitin, a protein with a single tyrosine, we showed that it is possible to determine the exact mol fractions (x_i) from the preexponential coefficients (A_i) associated with the decay times (τ_i) of the native (N) and unfolded (U) ubiquitin (5). In the case of ubiquitin, the native state was described by a single decay time, whereas two decay times were observed for the unfolded state. For RNase A, our experimental data show good fits with triple exponentials over the entire temperature range. This implies that the observed decay times are distributions of decay times of the native and unfolded states that are experimentally unresolved. However, the preexponential coefficients contain information on the mol fractions of the native folded (x_N) and unfolded (x_U) states. Thus, instead of the appearance of additional decay times, a change in the ratios of the preexponential coefficients is observed during the transition. Thermal and chemical unfolding both show a change in A_3 from ~4 to 2. This means that, when the protein is in the native state ($x_N = 1$) $A_3 = 4$, and when it is in the unfolded state ($x_N = 0$) $A_3 = 2$. Therefore, A_3 can be expressed in terms of the native molar fraction x_N (Eq. 12), from which the equilibrium constant for unfolding, K_U, can be determined and, in turn, the enthalpy (ΔH) and entropy (ΔS) of unfolding (Eq. 13).

$$A_3 = 2(x_N + 1) = 2((1 + K_U)^{-1} + 1). \quad (12)$$

$$K_U = (4 - A_3)/(A_3 - 2) = e^{-(\Delta H - T\Delta S)/RT}. \quad (13)$$

On fitting Eq. 13 to the temperature dependence of A_3, values of $T_m = 58.2$°C, $\Delta H = 461.4$ kJ/mol, and $\Delta S = 1.39$ kJ/mol/K were obtained (see Fig. 4 *b*). These values are in good agreement with previously published differential scanning calorimetry (DSC) results for thermal unfolding of RNase A at pH 5.5 ($T_m = 60.4$°C and $\Delta H = 453.4$ kJ/mol) (44).

Likewise, the GuHCl-induced unfolding provided values of $C_m = 2.93$ M, $\Delta G^{23^\circ C}_{H_2O} = 37.8$kJ/mol, and $m = 12.9$ kJ/mol/M, in reasonable agreement with values cited in the literature at pH 6.98: $C_m = 2.99$ M, $\Delta G^{25^\circ C}_{H_2O} = 38.7$kJ/mol, and $m = 12.9$ kJ/mol/M (45).

The interesting aspect of the agreement of the TRFS and DSC thermal unfolding results is that our TRFS values refer to thermal unfolding occurring in the regions of RNase A around Tyr-25 and Tyr-92, whereas the latter were derived from DSC measurements, thus reflecting the change in ΔC_p for the whole protein.

The picture emerging from this observation is that the unfolding of RNase A occurs via a ''domino effect'', in which all of the pieces undergo the transformation in a sequence but yet in one single process. Consistent with this picture is the fact that the T_m values derived from τ_1 vs. T (59.2°C), reflecting Tyr-76 (located on a loop between β-strands III and IV), from A_3 vs. T (58.2°C) for two tyrosine residues (Tyr-25, located on helix II, and Tyr-92, located on a loop between β-strands IV and V), from ΔA vs. T (62.2°C) reflecting the exposure to water of the three buried tyrosine residues (Tyr-25, Tyr-73, β-strand III, and Tyr-97, β-strand), and from DSC (60.4°C) (the whole protein) are all within the experimental DSC error (46).

Information on the unfolded conformation

There are several studies on the unfolded state of RNase A (for a review see Neira and Rico (6) and Scheraga et al. (7)) that indicate the presence of residual structure. This is confirmed by our results and expected from the presence of the four disulphide bridges, which prevent the complete expansion of the protein.

An interesting result of this work is that, of the four highly quenched Tyr residues, Tyr-73 and Tyr-97 remain in close proximity to their nearest disulphide bridges whereas Tyr-25 and Tyr-92 move away. Because the disulfide bridges nearest to Tyr-73 and Tyr-97 are located in secondary structures in regions of the protein different from the Tyr residues, this would tend to indicate that, at 80°C (above the $T_m \sim$ 60°C), tertiary contacts persist for Tyr-73 and Tyr-97.

On comparison of RNase A structures from the MD simulations at 23°C and 177°C, it is clear that the distance R between Tyr-25 and its nearest disulphide bridge Cys-26–Cys-84 results from the disruption of α-helix I, which causes the loop between α-helix I and α-helix II to shift toward α-helix I. In the case of Tyr-92 the partial loss in structure of β-strand V apparently causes an increase in the flexibility of the loop that contains Tyr-92, which results in a shift away from Cys-40–Cys-95.

Even more curious is the fact that, despite the partial loss in secondary structure of β-strand V, which contains Tyr-97, this strand still remains in close proximity to Cys-40–Cys-95. The C-terminal part of RNase A, which consists of Tyr-73 and Tyr-115, keeps its secondary structure, which maintains the two tyrosine residues in close proximity to their disulphide bridges. The last observation is in agreement with previous studies, which have indicated that Tyr-73 is located in a hydrophobic core of exceptional stability against unfolding.

CONCLUSIONS

The fluorescence decay of Ribonuclease A at pH 7 in the 20–80°C temperature range can be fit with triple-exponential decay functions despite the presence of six tyrosines. Below the unfolding temperature, four tyrosines are equally strongly quenched, one is partially quenched, and the sixth only slightly quenched. Upon unfolding two out of the four strongly quenched tyrosines become less quenched.

The quenching mechanism of these tyrosines in RNase A is ascribed to photo-induced electron transfer from the tyrosine residues to nearby disulphide bridges. The electron-transfer rate constant k_{ET} is exponentially dependent on the distance R from each tyrosine to the nearest disulphide bridge, using R-values obtained from the x-ray crystal structure and from the dynamic picture of the native and unfolded states provided by all-atom molecular dynamic simulations at 23, 87, and 177°C.

The three decay times were assigned as follows: τ_1 is the decay time of Tyr-76 (at $R = 12.8$ Å), τ_2 is the decay time of Tyr-115 (at $R = 6.9$ Å), and τ_3 is the mean decay time of Tyr-25, Tyr-73, Tyr-92, and Tyr-97 (all at $R = 5.5 \pm 0.3$ Å). Upon unfolding, the distances from two of the tyrosines (Tyr-25 and Tyr-92) to the nearest disulfide bridge increase from ~5.5 Å to ~7 Å and τ_2 becomes the average decay time of Tyr-115, Tyr-25, and Tyr-92, whereas τ_3 is the average decay time of Tyr-73 and Tyr-97.

From the preexponential coefficients of the fluorescence decays, the unfolding equilibrium constants (K_U) of RNase A were calculated, as a function of temperature or denaturant (GuHCl) concentration, providing values of $T_m = 58.2$°C and $C_m = 2.93$ M. The successful application of this method to the unfolding of RNase A rests on the fortunate case that, of the six tyrosine residues present, only two change significantly during unfolding.

This work establishes a new methodology of using TRFS as a tool for protein studies. The discrimination between and assignment of the six tyrosines allowed us to follow the unfolding in specific and different regions of the protein, evidencing an emerging picture of a single unfolding event that affects all the protein regions evenly.

In memory of his outstanding scientific and human qualities, and for being a source of inspiration for us, the authors dedicate this work to Prof. António V. Xavier who passed away on May 7, 2006.

The work was supported by the Fundação para a Ciência e a Tecnologia (FCT), Portugal, Projects POCI/QUI/56585/04 and POCI/BIA-PRO/57263/04 and by the European Commission, 5th Framework Program contract QLK3-CT-2000-00640. M. Noronha acknowledges a PhD grant from FCT, SRFH/BD/9096/2002.

REFERENCES

1. Royer, C. A. 2006. Probing protein folding and conformational changes with fluorescence. *Chem. Rev.* 106:1769–1784.
2. Beecham, J. M., and L. Brand. 1985. Time-resolved fluorescence of proteins. *Annu. Rev. Biochem.* 54:43–71.
3. Ferreira, S. T., L. Stella, and E. Gratton. 1994. Conformational dynamics of bovine Cu, Zn superoxide-dismutase revealed by time-resolved fluorescence spectroscopy of the single tyrosine residue. *Biophys. J.* 66:1185–1196.
4. Faria, T. Q., J. C. Lima, M. Bastos, A. L. Maçanita, and H. Santos. 2004. Protein stabilization by osmolytes from hyperthermophiles: effect of mannosylglycerate on the thermal unfolding of recombinant nuclease a from Staphylococcus aureus studied by picosecond time-resolved fluorescence and calorimetry. *J. Biol. Chem.* 279:48680–48691.
5. Noronha, M., J. C. Lima, M. Bastos, H. Santos, and A. L. Maçanita. 2004. Unfolding of ubiquitin studied by picosecond time-resolved fluorescence of the tyrosine residue. *Biophys. J.* 87:2609–2620.
6. Neira, J. L., and M. Rico. 1997. Folding studies on ribonuclease A, a model protein. *Fold. Des.* 2:R1–R11.
7. Scheraga, H. A., W. J. Wedemeyer, and E. Welker. 2001. Bovine pancreatic ribonuclease A: oxidative and conformational folding studies. *Methods Enzymol.* 341:189–221.
8. Navon, A., V. Ittah, J. H Laity, H. A. Scheraga, E. Haas, and E. E. Gussakovsky. 2001. Local and long-range interactions in the thermal unfolding transition of bovine pancreatic Ribonuclease A. *Biochemistry.* 40:93–104.
9. Noronha, M., J. C. Lima, P. Lamosa, H. Santos, C. Maycock, R. Ventura, and A. L. Maçanita. 2004. Intramolecular fluorescence quenching of tyrosine by the peptide carbonyl group revisited. *J. Phys. Chem. A.* 108:2155–2166.
10. Giestas, L., C. Yihwa, J. C. Lima, C. Vantier-Giongo, A. Lopes, A. L. Maçanita, and F. H. Quina. 2003. The dynamics of ultrafast excited state proton transfer in anionic micelles. *J. Phys. Chem. A.* 107:3263–3269.
11. Striker, G., V. Subramaniam, C. A. M. Seidel, and A. J. Volkmer. 1999. Photochromicity and fluorescence lifetimes of green fluorescent protein. *J. Phys. Chem. B.* 103:8612–8617.
12. Ferreira da Silva, P., J. C. Lima, F. H. Quina, and A. L. Maçanita. 2004. Excited-state electron transfer in anthocyanins and related flavylium salts. *J. Phys. Chem. A.* 108:10133–10140.
13. HyperchemTM. Release 6.01 for Windows. 2000. Hypercube, Gainesville, FL.
14. Brooks, B. R., R. E. Bruccoleri, B. D. Olafson, D. J. States, S. Swaminathan, and M. Karplus. 1983. Charmm—a program for macromolecular energy, minimization, and dynamics calculations. *J. Comput. Chem.* 4:187–217.
15. MacKerell, A. D. Jr., D. Bashford, M. Bellotand, R. L. Dunbrack Jr., J. D. Evanseck, M. J. Field, S. Fischer, J. Gao, H. Guo, S. Ha, D. Joseph-McCarthy, L. Kuchnir, et al. 1998. All-atom empirical potential for molecular modelling and dynamics studies of proteins. *J. Phys. Chem. B.* 102:3586–3616.
16. Im, W., M. S. Lee, and C. L. Brooks. 2003. Generalized born model with a simple smoothing function. *J. Comp. Chem.* 24:1691–1702.
17. Chatani, E., R. Hayashi, H. Moriyama, and T. Ueki. 2002. Conformational strictness required for maximum activity and stability of bovine pancreatic ribonuclease A as revealed by crystallographic study of three Phe120 mutants at 1.4 Å resolution. *Protein Sci.* 11: 72–81.
18. Cowgill, R. W. 1964. Fluorescence and the structure of proteins III. Effects of denaturation on fluorescence of insulin and ribonuclease. *Arch. Biochem. Biophys.* 104:84–92.
19. Willis, K. J., and A. G. Szabo. 1991. Fluorescence decay kinetics of tyrosinate and tyrosine hydrogen-bonded complexes. *J. Phys. Chem.* 95:1585–1589.
20. Markley, J. L. 1975. Correlation proton magnetic resonance studies at 250 MHz of bovine pancreatic ribonuclease. II. pH and inhibitor-induced conformational transitions affecting histidine-48 and one tyrosine residue of ribonuclease A. *Biochemistry.* 14:3554–3561.
21. Gally, J. A., and G. M. Edelman. 1962. Effect of temperature on fluorescence of some aromatic amino acids and proteins. *Biochim. Biophys. Acta.* 60:499–509.
22. Santoro, J., C. Gonzalez, M. Bruix, J. L. Neira, J. L. Nieto, J. Herranz, and M. Rico. 1993. High-resolution 3-dimensional structure of ribonuclease-A in solution by nuclear-magnetic-resonance spectroscopy. *J. Mol. Biol.* 229:722–734.
23. Hermans, J., Jr., and H. A. Scheraga. 1961. Structural studies of ribonuclease. 5. Reversible change of configuration. *J. Am. Chem. Soc.* 83: 3283–3292.
24. Cowgill, R. W. 1966. Relationship between tyrosine fluorescence and various stages in denaturation of ribonuclease. *Biochim. Biophys. Acta.* 120:196–211.
25. Cowgill, R. W. 1976. Tyrosyl fluorescence in proteins and model proteins. *In* Biochemical Fluorescence: Concepts, Vol. 2. R. F. Chen and H. Edelhoch, editors. Marcel Dekker, New York and Basel, Switzerland.
26. Swadesh, J. E., P. W. Mui, and H. A. Scheraga. 1987. Thermodynamics of the quenching of tyrosyl fluorescence by dithiothretiol. *Biochemistry.* 26:5761–5769.
27. Chen, Y., and M. D. Barkley. 1998. Towards understanding tryptophan fluorescence in proteins. *Biochemistry.* 37:9976–9982.
28. Schafferman, A., and G. Stein. 1974. The effect of aromatic amino acids on the photochemistry of a disulphide; energy transfer and reaction with hydrated electrons. *Photochem. Photobiol.* 20:399–406.
29. Cowgill, R. W. 1967. Fluorescence and protein structure. 11. Fluorescence quenching by disulfide and sulfhydryl groups. *Biochim. Biophys. Acta.* 140:37–44.
30. Cowgill, R. W. 1964. Fluorescence and structure of proteins. 3. Effects of denaturation on fluorescence of insulin and ribonuclease. *Arch. Biochem. Biophys.* 104:84–92.
31. Seidel, C., A. Orth, and K. O. Greulich. 1993. Electronic effects on the fluorescence of tyrosine in small peptides. *Photochem. Photobiol.* 58: 178–184.
32. Gorin, G., and G. Doughty. 1968. Equilibrium constants for the reaction of glutathione with cystine and their relative oxidation-reduction potentials. *Arch. Biochem. Biophys.* 126:547–551.
33. Weller, A. 1982. Photo-induced electron transfer in solution: exciplex and radical ion pair formation free enthalpies and their solvent dependence. *Z. Phys. Chem. N. F.* 133:93–98.
34. Schwartz, R. L., G. E. Davico, and W. C. Lineberger. 2000. Negative-ion photoelectron spectroscopy of CH3S–. *Journal of Electron Spectroscopy and Related Phenomena.* 108:163–168.
35. Janousek, B. K., K. J. Reed, and J. I. Brauman. 1980. Electron photodetachment from mercaptyl anions (RS-). Electron affinities of mercaptyl radicals and the sulfur-hydrogen bond strength in mercaptans. *J. Am. Chem. Soc.* 102:3125–3129.
36. Marcus, R. A. 1960. Theory of oxidation-reduction reactions involving electron transfer. 4. A statistical-mechanical basis for treating contributions from solvent, ligands, and inert salt. *Discuss. Faraday Soc.* 29: 21–31.
37. Marcus, R. A. 1993. Electron-transfer reactions in chemistry-theory and experiment (Nobel lecture). *Angew. Chem. Int. Ed. Engl.* 32:1111–1121.
38. Marcus, R. A., and N. Sutin. 1985. Electron transfers in chemistry and biology. *Biochim. Biophys. Acta.* 811:265–322.
39. Chen, P., R. Duesing, D. K. Graff, and T. J. Meyer. 1991. Intramolecular electron transfer in the inverted region. *J. Phys. Chem.* 95: 5850–5858.
40. Liu, T., P. R. Callis, B. H. Hesp, M. de Groot, W. J. Buma, and J. Broos. 2005. Ionization potentials of fluoroindoles and the origin of

nonexponential tryptophan fluorescence decay in proteins. *J. Am. Chem. Soc.* 127:4104–4113.

41. Reference deleted in proof.
42. Page, C. C., C. C. Moser, X. Chen, and P. L. Dutton. 1999. Natural engineering principles of electron tunneling in biological oxidation-reduction. *Nature*. 402:47–52.
43. Costa, S. M. B., A. L. Maçanita, and S. J. Formosinho. 1984. Effective distances of exothermic charge-transfer reactions in the excited state. *J. Phys. Chem.* 88:4089–4095.
44. Xie, G., and S. N. Timasheff. 1997. Mechanism of the stabilization of ribonuclease A by sorbitol: preferential hydration is greater for the denatured than for the native protein. *Protein Sci.* 6:211–221.
45. Pace, C. N., D. V. Laurents, and J. A. Thomson. 1990. pH dependence of the urea and guanidine hydrochloride denaturation of ribonuclease A and ribonuclease T1. *Biochemistry.* 29:2564–2572.
46. Hinz, H. J., and F. P. Schwartz. 2001. Measurement and analysis of results obtained on biological substances with differential scanning calorimetry. *Pure Appl. Chem.* 73:745–759.